Energy spectrum of primary cosmic rays between $10^{14.5}$ and 10^{18} eV

1984 J. Phys. G: Nucl. Phys. 10 1295

(http://iopscience.iop.org/0305-4616/10/9/016)

J. Phys. G: Nucl. Phys. 10 (1984) 1295–1310. Printed in Great Britain

Energy spectrum of primary cosmic rays between $10^{14.5}$ and 10^{18} eV

M Nagano†, T Hara†, Y Hatano†, N Hayashida†, S Kawaguchi‡, K Kamata†, T Kifune† and Y Mizumoto§

† Institute for Cosmic Ray Research, University of Tokyo, Midoricho, Tanashi, Tokyo 188, Japan
‡ Faculty of General Education, Hirosaki University, Bunkyocho, Hirosaki 036, Japan
§ Department of Physics, University of Utah, Salt Lake City, Utah 84112, USA

Received 17 January 1984

Abstract. Size spectra of electrons (N_e) and muons (N_μ) are obtained from the Akeno extensive air-shower experiment. The primary spectrum estimated from each spectrum is the same and is expressed by $J(E_0)\,dE_0(4.0–5.0)\times 10^{-23}(E_0/10^{15.67})^{-\gamma}\,dE_0\ \mathrm{m^{-2}\,s^{-1}\,sr^{-1}}$ where $\gamma=2.62\pm0.12$ below and $\gamma=3.02\pm0.05$ above $10^{15.67}$ eV. There is no other significant change of slope in either the electron or the muon size spectrum beyond the corresponding energy $10^{15.67}$ eV.

1. Introduction

The detailed study of the energy spectrum of primary cosmic rays between $10^{14.5}$ and 10^{18} eV is important in relation to the origin and propagation of cosmic rays in the Galaxy. If the sources of cosmic rays in this energy region are in the galactic disc, and if more than two kinds of nuclei are mixed, the energy spectrum of each nucleus can be modified according to its rigidity in an interstellar magnetic field. The steepening of the spectrum at a few times 10^{15} eV (the 'knee') can be interpreted as evidence for a leakage from the trapping zone of the cosmic rays (see, e.g., Hillas 1981). In this case we expect another structure above 10^{16} eV in the primary energy spectrum depending on the features of the mixing of compositions. An alternative explanation of the 'knee' is based on the possibility of the limitation in the acceleration process at the source and is not related to trajectories in a magnetic field (Hillas 1979). Furthermore, it is probable that the contribution of extragalactic cosmic rays exceeds that of galactic origin somewhere above 10^{17} eV so that the slope of the spectrum may change. Though many measurements of the energy spectrum below 10^{16} and above 10^{18} eV have been reported (Grigorov *et al* 1971, Danilova *et al* 1977, Bower *et al* 1981, Efimov *et al* 1981, Kirov *et al* 1981), relatively few have been performed between 10^{16} and 10^{18} eV (Lapointe *et al* 1968, Kakimoto *et al* 1981) and no convincing structure has yet been reported.

Another interest in the primary spectrum is related to the difference in the primary spectra derived from the electron and muon components (Kakimoto *et al* 1981). Agreement between these spectra is necessary and the conditions for the agreement require important constraints on the model of hadronic interaction as well as primary composition.

In this paper we present a detailed study of the size spectra of electrons and muons determined using more than 50 000 showers selected from 300 000 analysed showers which were observed by the Akeno extensive air-shower array between 1979 and the spring of 1983. Since the electron size and muon size of individual showers are determined with fairly good accuracy, we try to detect if any change of spectrum shape, in either electrons or muons or both, exists. The primary energy spectrum between $10^{14.5}$ and 10^{18} eV is derived from the present electron size spectrum using the longitudinal development curve observed at Chacaltaya (Kakimoto *et al* 1981). The spectrum is also derived from the muon size spectrum after establishing the relation between the muon size and the particle density measured by a scintillator at 600 m from the core. Since both conversion methods from size spectra to energy spectrum are accepted to be insensitive to the interaction models and to primary composition, the primary spectra derived from the electron size spectrum and the muon size spectrum are expected to be in agreement.

2. Experiment

The Akeno air-shower array is described by Hara *et al* (1979). The electron size is determined with 150 scintillation detectors of area 1 m^2 each and 6 scintillation detectors of area 2 m^2 each, deployed over an area of roughly 1 km^2. For the observation of showers of less than 10^7 particles, detectors of areas 0.25 and 0.02 m^2 arranged in the central part of the array are also used. The muon size is determined with nine stations of proportional counter arrays of area 25 m^2 each. The threshold muon energy varies with the zenith angle θ and is given by 1 GeV $\times$ sec θ.

Experiments with five different triggering requirements (A, B, C, D and E) were carried out in order to cover the broad size range with sufficient statistics. The details of the experiments and the analysis procedure are described by Nagano *et al* (1984, hereafter referred to as I). The numbers of triggered showers, analysed showers and selected showers used to construct the spectrum reported here are listed in table 1, together with the triggering requirement, the effective area and observation time. An example of the lateral distribution of electrons and muons in a typical shower is shown in figure 1.

The electron size (N_e) is determined by fitting the particle densities measured by scintillators of thickness 50 mm to the NKG formula of variable age (Greisen 1968).

A modified version of the Greisen formula (Hara *et al* 1983a) is used for the lateral distribution of muons (LDM):

$$\rho_\mu = \frac{\Gamma(2.5)}{2\pi\Gamma(1.25)\Gamma(1.25)} R_0^{-1.25} N_\mu r^{-0.75}(1 + r/R_0)^{-2.5} \qquad r \geqslant 50 \text{ m} \qquad (1)$$

where $R_0 = 280$ m independent of zenith angle. To determine the muon size of each shower, only the muon stations beyond 100 m from the core are used for the trigger E, but those between 50 and 200 m are used for the triggers A–D.

In constructing the size spectrum the showers whose cores hit the area of 100% detection efficiency are selected. This area is determined by plotting the core positions on the map in each size, zenith-angle and age bin and then selecting the region where the cores are distributed uniformly. These areas are also estimated by analysing artificial showers with the average lateral distribution and fluctuation of density as described later. An example of the estimated efficiency is shown for trigger E as a function of shower age and N_e in figure 2.

Table 1. Experimental conditions.

Experiment	Trigger	Serial number	Triggering requirement	Effective area	Threshold size	Observation time (s)	Number of triggered events	Number of analysed events	Number of selected events
II	A	211–225	$\left.\begin{matrix} S2106 \geqslant 1 \\ S2107 \geqslant 1 \\ S2110 \geqslant 1 \\ S2111 \geqslant 1 \\ S2124 \geqslant 10 \end{matrix}\right\}$ 5F	15 m^r	1.0×10^5	9.08×10^5	16250	11418	1973
	B	367–373	$\left.\begin{matrix} S2106 \geqslant 4 \\ S2107 \geqslant 4 \\ S2110 \geqslant 4 \\ S2111 \geqslant 4 \\ S2124 \geqslant 10 \\ S2132 \geqslant 4 \end{matrix}\right\}$ 6F	30 m^r	2.0×10^5	8.76×10^5	10230	6307	916
	C	190–462	$\left.\begin{matrix} S2106 \geqslant 10 \\ S2107 \geqslant 10 \\ S2110 \geqslant 10 \\ S2111 \geqslant 10 \end{matrix}\right\}$ 4F	30 m^r	1.0×10^6	3.21×10^7	75000	45414	10777
	D	469–675	$\left.\begin{matrix} S2106 \geqslant 15 \\ S2107 \geqslant 15 \\ S2110 \geqslant 15 \\ S2111 \geqslant 15 \end{matrix}\right\}$ 4F	30 m^r	2.0×10^6	3.63×10^7	80000	49524	17375
III	E	274–670	Any 7 out of 38 detectors deployed over 1 km^2 (each $\geqslant 4$)	$400 \times 500\ m^2$	1.0×10^7	6.15×10^7	254000	198330	23400

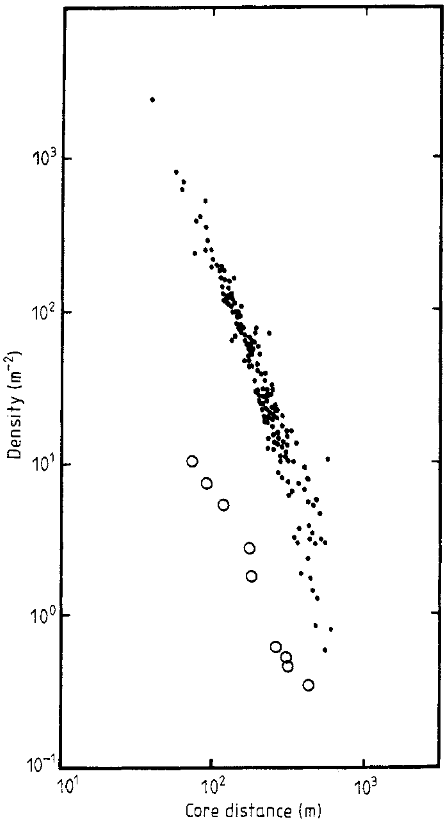

Figure 1. An example of the lateral distribution of electrons (●) and muons (○) in a typical shower. ($N_e = 6.4 \times 10^7$; $N_\mu = 1.8 \times 10^6$; zenith angle 34°.)

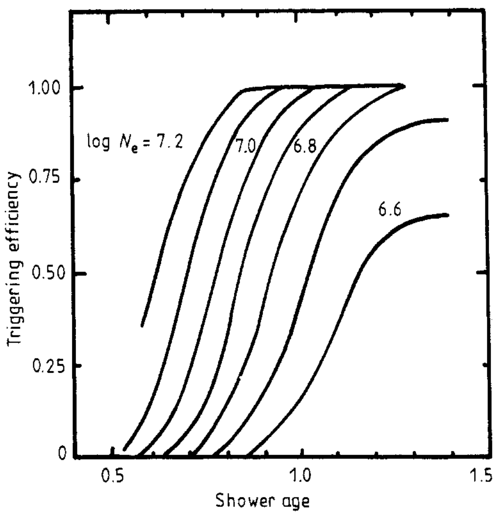

Figure 2. Calculated efficiency for triggering requirement E as a function of age and electron size.

3. Results

3.1. Electron size spectra at different zenith angles

As described in I, the lateral distribution of electrons (LDE) cannot be fitted to the NKG function of constant age over the whole distance range. If we determine a local age parameter (LAP) by fitting the NKG function to densities in some core distance ranges then the LAP varies with core distance, that is, the shower age and N_e of the same shower are assigned to the different values depending on the core distance ranges when they are observed by the different shower arrays. Furthermore, the densities measured by scintillators of thickness 50 mm show a transition effect near the core. In the following we derive the true N_e from the calculated N_e^c with the present analysis procedure.

3.1.1. Definition of a 'single electron'. We define a 'single electron' by the average of the pulse-height distribution of muons traversing vertically a scintillator of thickness 3 mm (about 0.5 MeV energy loss). Muons traversing vertically were selected by two small scintillators (area 0.02 m^2), separated by 1 m in height, which were surrounded by scintillators to discriminate against local showers. However, we commonly use a single 'particle' which corresponds to a peak of the pulse-height distribution of omnidirectional muons for the convenience of detector maintenance. This value corresponds to 1.1 'electrons', and hence it is necessary to decrease N_e^c systematically by 10%.

3.1.2. Transition effect in a detector and the flattening of the LDE far from the core. Since there is a transition effect in a scintillator of thickness 50 mm and its container near the core, the size is, in general, overestimated. On the other hand, the NKG formula which is fitted to the densities near the core predicts lower values than are observed far from the core and hence the size is underestimated. By accident both effects compensate for each other in the size estimation described in I, that is, the size fitted to the densities measured by a 50 mm scintillator within 100 m and that fitted to the densities outside 100 m give almost the same size, in spite of the different ages assigned. The slight difference between them is estimated in § 3.1.3.

3.1.3. Correction of size spectra due to the dispersion in size determination. The observed fluxes in each size bin are increased by the factor $f_c = \exp(\frac{1}{2}\alpha^2\gamma^2)$ where γ is the exponent of the size spectrum and α is the standard deviation in the size determination on a logarithmic scale (Kiraly *et al* 1971). Here we assume uncertainties in size determination which are symmetrical on a logarithmic scale and which are gaussian distributions. In order to find $\alpha(N_e)$ sets of showers have been simulated by a Monte-Carlo method and subjected to the normal analysis. The following function and the observed density fluctuation around the average are used for the simulation:

$$f(r) = C_1 X^{S-2}(1+X)^{S-4.5}(1+C_2 X^d) \qquad (2)$$

where $X = r/r_0$ and C_1 is a normalisation factor given in terms of the beta function by

$$C_1 = N_e/2\pi r_0 (B(S, 4.5-2S) + C_2 B(S+d, 4.5-d-2S))^{-1}.$$

We use $d = 1.3$ and $C_2 = 0.2$. The output/input size ratio ($R_N = N_{\text{output}}/N_{\text{input}}$) and values of f_c are tabulated in table 2 for the case of trigger E. Since the assumed function (2) is obtained by fitting to the densities measured by a 50 mm thick scintillator throughout the

Table 2. The output/input size ratio (R_N) and the overestimation factor f_c increased due to the uncertainty in electron size determination for trigger E.

$\log N_e$	θ	S	$R_N = N_{output}/N_{input}$	f_c
7.0	17	0.95	0.93 ± 0.01	1.13
7.5	17	0.95	0.93 ± 0.01	1.10
8.0	17	0.95	0.91 ± 0.01	1.09
8.5	17	0.95	0.89 ± 0.01	1.06
7.0	30	1.0	0.95 ± 0.01	1.10
7.5	30	1.0	0.94 ± 0.01	1.07
8.0	30	1.0	0.90 ± 0.01	1.06
8.5	30	1.0	0.88 ± 0.01	1.05
7.0	37	1.05	0.94 ± 0.01	1.08
7.5	37	1.05	0.95 ± 0.01	1.06
8.0	37	1.05	0.92 ± 0.01	1.06
8.5	37	1.05	0.90 ± 0.01	1.04
7.0	42	1.1	0.95 ± 0.01	1.07
7.5	42	1.1	0.93 ± 0.01	1.05
8.0	42	1.1	0.91 ± 0.01	1.04
8.5	42	1.1	0.89 ± 0.01	1.04
7.0	50	1.15	0.93 ± 0.01	1.05
7.5	50	1.15	0.92 ± 0.01	1.04
8.0	50	1.15	0.90 ± 0.01	1.03
8.5	50	1.15	0.88 ± 0.01	1.03

core distance range, N_{input} is 10% larger than the true N_e due to the transition effect near the core.

Taking the factors R_N, f_c and the ratio N_{input}/N_e, into account the correction factor to the size due to §§3.1.2 and 3.1.3 is (-13 to -2)% in the size range $10^{7.0}$–$10^{8.5}$ and the sec θ range 1.0–1.5. For triggers A–D this correction is less than about 3% and is hence neglected.

3.1.4. Correction for dispersion in zenith-angle determination. The measured fluxes at large zenith angles are increased by the contamination of showers of smaller incident zenith angles due to the error in the determination of arrival directions. This correction was calculated numerically by assuming a gaussian distribution with standard deviation of $\sigma(\theta)$. The factor of overestimation (f_θ) depends on the value of $\sigma(\theta)$; some values are listed in table 3 as a function of zenith angle for trigger E. For triggers A–D $\sigma(\theta)$ is less than 2.5° for $\theta < 50°$ and the correction can be neglected.

The differential size spectra after allowing for the above corrections are derived for three effective areas for triggers A and B (314, 706 and 1960 m^2) and C and D (256, 900 and 3600 m^2) and two effective areas for trigger E (20 000 and 42 000 m^2). By comparing

Table 3. The overestimation factor f_θ due to the uncertainty in zenith-angle determination for trigger E.

sec θ	1.0	1.1	1.2	1.3	1.4	1.5	1.6
f_θ	0.98	0.98	1.03	1.08	1.17	1.27	1.48

the spectra obtained, statistically significant values are chosen in overlapping size regions which ensure the triggering efficiency is 100%. The differential size spectra of electrons obtained are shown in figure 3. The bars represent statistical errors only. The differential spectra at various zenith angles are expressed by the equation

$$J_e(N_e, \theta)\, dN_e = A_e(\theta)(N_e/10^6)^{-\gamma_e(\theta)}\, dN_e.$$

Values of $\gamma_e(\theta)$ below and above 10^6 are listed in table 4 together with the flux at 10^6 ($A_e(\theta)$).

The kink at 10^6 is clearly seen in the vertical direction but becomes less distinct as the zenith angle increases. There is no other significant change of slope up to $10^{8.0}$.

3.2. Muon size spectra

Muon sizes were determined with the LDM function (1) with $R_0 = 280$ m. The LDM depends on zenith angle and the parameter R_0 increases as the zenith angle increases (Hara *et al* 1983a). In the following we determine the vertical muon size spectrum; its zenith-angle dependence will be described in a separate paper.

3.2.1. Correction of outputs from proportional counters to the 'muon' number. The density (ρ_μ) averaged over the responses of 50 proportional counters are calibrated with the number of tracks (n_μ) counted by three-layer arrays of proportional counters which are installed in two of the muon stations. The ratio of the total responses of 50 proportional

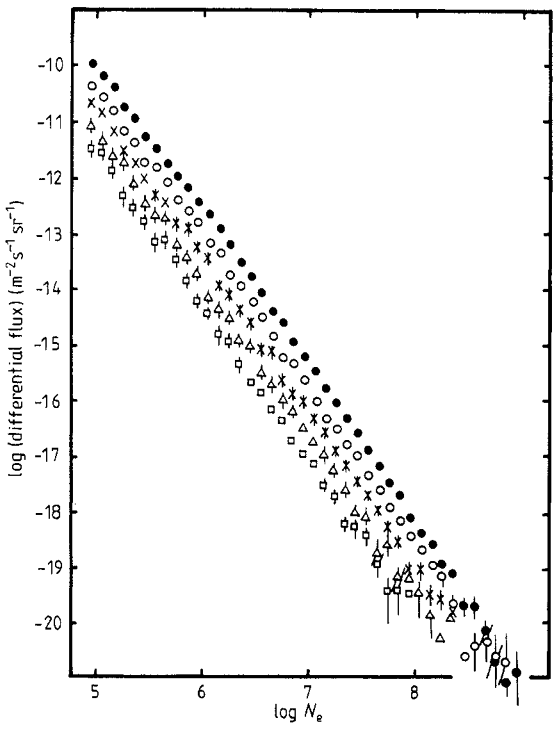

Figure 3. The differential electron size spectra at five zenith angles: sec θ = 1.0 (●), 1.1 (○), 1.2 (×), 1.3 (△) and 1.4 (□).

Table 4. Exponents γ and fluxes at 10^6 in electron size spectra.

sec θ	$10^{5.0}$–$10^{6.0}$	$10^{6.0}$–$10^{8.0}$	Flux at $10^{6.0}$ ($m^{-2}\,s^{-1}\,sr^{-1}$)
1.0	-2.48 ± 0.09	-2.83 ± 0.04	$(2.80 \pm 0.08) \times 10^{-13}$
1.1	-2.49 ± 0.17	-2.80 ± 0.12	$(1.2 \pm 0.2) \times 10^{-13}$
1.2	-2.59 ± 0.19	-2.74 ± 0.08	$(3.8 \pm 0.7) \times 10^{-14}$
1.3	-2.63 ± 0.26	-2.57 ± 0.22	$(1.2 \pm 0.3) \times 10^{-14}$
1.4	-2.73 ± 0.32	-2.62 ± 0.20	$(5.0 \pm 0.8) \times 10^{-15}$

counters to n_μ varies with core distance and is listed in table 5. The increase in the ratio near the core can be explained by the effect of knock-on and bremmstrahlung processes (Jogo 1981). An independent calibration with a hodoscope of neon flash tubes gives almost the same value (Jogo 1981).

3.2.2. Correction of size spectra due to the dispersion in the determination of muon size. For muon spectra $\sigma(N_\mu)$ is related to N_μ and the corresponding f_c are listed in table 6. The differential muon size spectrum between sec $\theta = 1.0$ and 1.1 is shown in figure 4. The triggering of the present experiment is made by scintillation detectors on the surface so that the non-biased region of 100% detection efficiency for muon size is selected via the N_μ against N_e diagram for each trigger. Direct triggering by muons was started in 1982 and the result will be reported in the near future.

The differential muon size spectrum in the vertical direction is expressed by the equation

$$J_\mu(N_\mu)\,dN_\mu = A_\mu(N_\mu/10^6)^{-\gamma}\,dN_\mu$$

where $\gamma = 3.44 \pm 0.09$ and $A_\mu = (3.08 \pm 0.17) \times 10^{-16}\ m^{-2}\,s^{-1}\,sr^{-1}$ between 10^5 and $10^{6.7}$.

4. Discussion

4.1. Comparison of the N_e spectrum with other observations and longitudinal development of electrons from equi-intensity cuts

The vertical integral N_e spectra obtained by other groups are compared with the present ones for sec $\theta = 1.0$ and 1.1 in figure 5. In the figure the fluxes multiplied by N_e^2 are drawn on the vertical axis to emphasise the spectral shape. For comparison of our data with those at higher altitude, the longitudinal development curve from equi-intensity cuts of integral size spectra at various zenith angles are plotted in figure 6 together with other experiments. Our spectrum at sec $\theta = 1.1$ corresponds to an atmospheric depth of 1020 g cm^{-2} and

Table 5. The ratio of the total responses of 50 proportional counters to the number of tracks counted by a three-layer proportional counter array as a function of core distance.

r(m)	50	60	70	80	90	100
ρ_μ/n_μ	1.85	1.85	1.75	1.68	1.65	1.6

Table 6. The overestimation factor f_c due to the uncertainty in muon size determination.

Trigger								
A–D	$\log N_\mu$	5.0	5.2	5.4	5.6			
	f_c	1.42	1.40	1.38	1.36			
E	$\log N_\mu$	5.8	6.0	6.2	6.4	6.6	6.8	
	f_c	1.22	1.21	1.2	1.19	1.18	1.18	

hence should be compared with those at sea level. It is remarkable that the spectra of all groups except that at Kobe University (Asakimori *et al* 1982) show the 'knee' around 10^6 irrespective of observation level with almost the same slope below the 'knee'. The absolute values obtained by the Moscow University group (Vernov *et al* 1968) agree with ours within experimental errors, but those of the KGF (920 g cm^{-2}; Acharya *et al* 1981) and Kiel University groups (Bagge *et al* 1977) do not agree with ours. The reason why the KGF group obtains a low flux may be that they do not take the zenith angle into account in their shower analysis. Their flux should be increased at least by a factor of 1.33 due to the difference in the zenith-angle distribution. (They used $\cos^7\theta$ instead of the present $\cos^{10}\theta$ dependence to derive the vertical flux from the omnidirectional size spectrum.) The slopes above the 'knee' of the KGF, Moscow and Kiel spectra are different from the present experiment. However, their fluxes at their highest sizes are so low that they do not disagree with our data within their statistical errors.

From figures 5 and 6 we see that the flux of the present experiment is intermediate between the data from Chacaltaya (Kakimoto *et al* 1981) and Norikura (Kawakami *et al* 1983) on the one hand, and those from Tien-Shan (Kirov *et al* 1981), Yakutsk (Diminstein

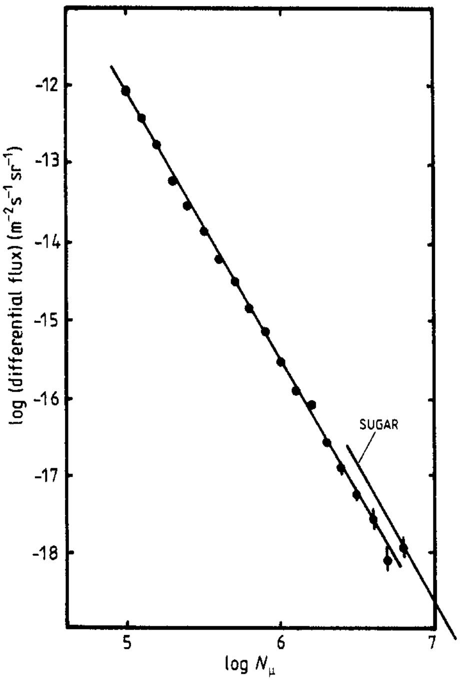

Figure 4. The differential muon size spectrum at sec θ = 1.0–1.1. The results of the SUGAR experiment (Horton *et al* 1983) is also shown.

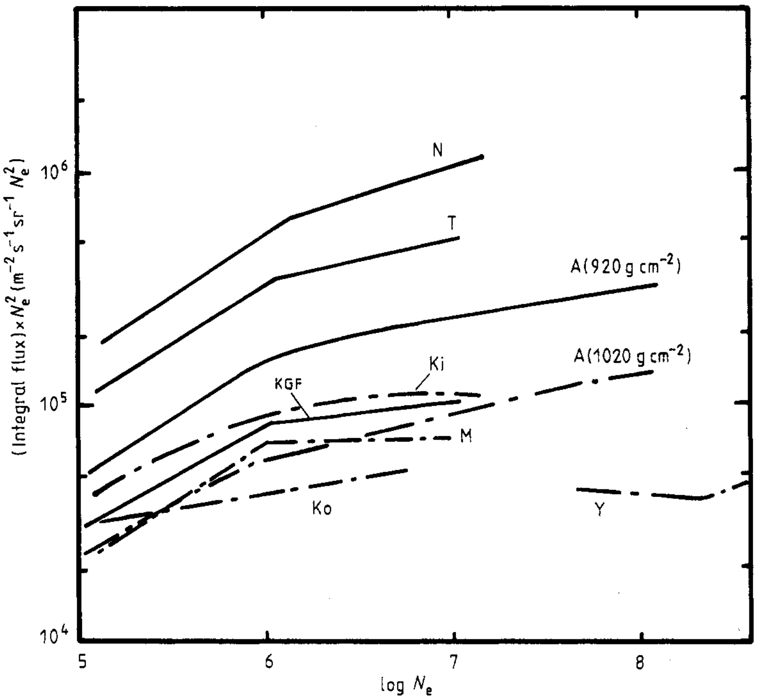

Figure 5. The vertical integral N_e spectra of other groups are compared with the present ones with sec $\theta = 1.0$ and 1.1 (A): N, Norikura (740 g cm^{-2}; Kawakami *et al* 1983); T, Tien-Shan (690 g cm^{-2}; Kirov *et al* 1981); KGF (920 g cm^{-2}; Acharya *et al* 1981); Ko, Kobe University (sea level; Asakimori *et al* 1982); M, Moscow State University (sea level; Vernov *et al* 1968); Ki, Kiel University (sea level; Bagge *et al* 1977); Y, Yakutsk (sea level; Diminstein *et al* 1977).

et al 1977) and Volcano Ranch (Linsley 1973) on the other. One of the reasons for the differences among the groups may be the differences in detector arrangement. Since the LDE cannot be described by a single value of the age parameter over a large range of distances as described in I, different values of size and age are obtained for the same shower depending on which range of core distances the lateral distribution is fitted in.

4.2. Comparison of the N_μ spectrum with other observations

In figure 4 the present result is compared with the revised spectrum of the SUGAR experiment (Horton *et al* 1983). There is a systematic difference of 25% in muon size. Considering the difference in the threshold energy between Sydney (0.75 GeV) and ours (1 GeV), the difference is not serious. If we normalise both spectra to each other, there is no change of slope in the muon size spectrum between 10^5 and 10^9.

4.3. Primary energy spectrum from N_e

The electron size at the maximum of shower development is well known as one of the best primary energy estimators which does not depend sensitively on the interaction model or primary composition. We estimate this quantity with the help of the longitudinal development curve measured at Chacaltaya (Kakimoto *et al* 1981) as shown in figure 6.

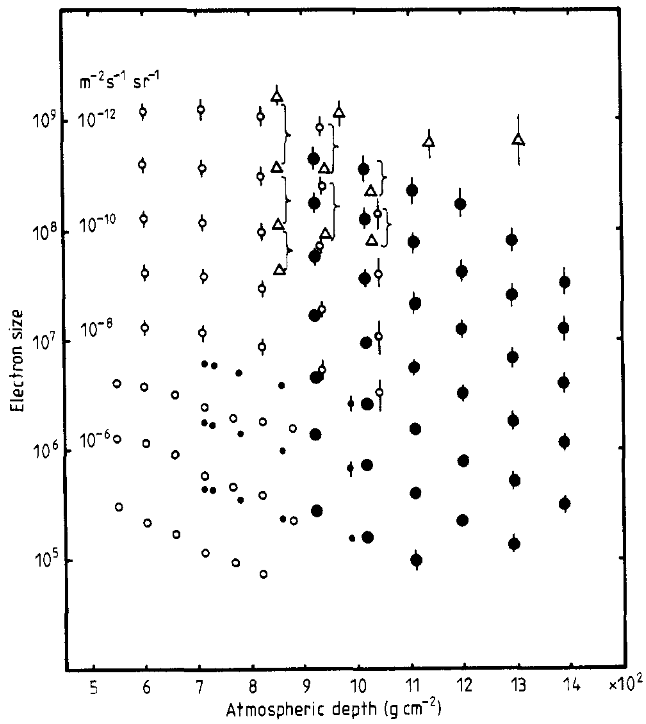

Figure 6. The longitudinal development curve from equi-intensity cuts of integral spectra at various zenith angles: ●, present results; ○, Chacaltaya (Kakimoto *et al* 1981); •, Tien-Shan (Kirov *et al* 1981); △, Volcano Ranch (Linsley 1973).

The ratios $R(\max/920)$ of shower size at maximum ($N_e(\max)$) to size at 920 g cm^{-2} ($N_e(920)$) of their measurement are listed in table 7 for the five constant fluxes.

By multiplying our vertical size ($N_e(920)$) by this ratio, $N_e(\max)$ from our experiment is estimated and listed in column 4 in table 7. The energies at the corresponding fluxes are obtained by multiplying this size by the conversion factor (w) from $N_e(\max)$ to E_0. According to Hillas (1983), the following conversion factor w is most plausible in the case of a rising hadron–air-nucleus cross section whose energy dependence is consistent with our recent result (Hara *et al* 1983b): $w = 1.4$ GeV for $3 \times 10^6 \leqslant N_e < 10^{10}$, $w = 1.45$ GeV at $N_e = 10^6$ and $w = 1.59$ GeV at $N_e = 10^5$. When these values are applied we get the conversion factor u from the size at Akeno to E_0, as shown in figure 7, by extrapolating the

Table 7. The conversion factor u from the size at Akeno to E_0 via the longitudinal development curve measured at Chacaltaya.

Integral flux ($m^{-2}\,s^{-1}\,sr^{-1}$)	$R(\max/920)$ Chacaltaya	$N_e(920)$ Akeno	$N_e(\max)$ from Akeno	E_0 (eV)	From $N_e(920)$ to E_0 (GeV)
10^{-12}	1.47 ± 0.64	4.5×10^8	6.62×10^8	9.26×10^{17}	2.06 ± 0.90
10^{-11}	1.67 ± 0.47	1.8×10^8	3.01×10^8	4.21×10^{17}	2.34 ± 0.65
10^{-10}	1.85 ± 0.48	5.8×10^7	1.07×10^8	1.50×10^{17}	2.59 ± 0.67
10^{-9}	2.10 ± 0.59	1.7×10^7	3.57×10^7	5.00×10^{16}	2.94 ± 0.82
10^{-8}	2.41 ± 0.53	4.6×10^6	1.11×10^7	1.55×10^{16}	3.37 ± 0.74

ratio $R(\max/920)$ to lower sizes. By using these conversion factors the differential spectrum obtained between $10^{14.7}$ and 10^{18} eV is added to the earlier results compiled by Hillas (1983) in figure 8.

4.4. Primary energy spectrum from N_μ spectrum

Since the attenuation of N_μ is very small after the maximum of shower development, N_μ is a good estimator of primary energy. However, the conversion factor depends sensitively on the interaction model and composition. Therefore it is necessary to estimate N_μ/E_0 with the help of other experiments. The Haverah Park group showed that the signal measured by a deep-water Cerenkov tank at 600 m from the core ($\rho(600)$) is a good measure of primary energy, independent of interaction model and composition, from detailed simulations (see Bower *et al* 1983) and these quantities are related by

$$E_0(\mathrm{eV}) = (7.04 \times 10^{17})\, \rho(600)^{1.018}.$$

The ratio $\rho(600)$ to the density measured by the scintillator at 600 m ($S(600)$) obtained by the Haverah Park group is 0.47 (Bower *et al* 1983) and hence

$$E_0(\mathrm{eV}) = (3.26 \times 10^{17})\, S(600)^{1.018}. \qquad \text{(HP)}$$

On the other hand, the Yakutsk group derived a relation between E_0 and $S(600)$ via the total Cerenkov photon flux from EAS (Glushkov *et al* 1979) which gives

$$E_0(\mathrm{eV}) = (4.1 \pm 1.5) \times 10^{17}\, S(600)^{0.96}. \qquad \text{(Y)}$$

Figure 9 shows the lateral distributions of electrons of various sizes at a fixed N_μ observed at Akeno. The proportion of fluxes for each N_e range is also listed in the figure. It is found that the dispersion of $S(600)$ is about half that of N_e for a fixed N_μ. The relation between N_μ and $S(600)$ at a depth corresponding to sea level is expressed by

$$S(600) = (0.34 \pm 0.03)\, (N_\mu/10^6)^{1.20 \pm 0.05}$$

for $10^{5.5} \leqslant N_\mu < 10^{6.3}$. By extrapolating the above relation to lower values of $S(600)$ and by neglecting the muon size attenuation between Akeno and sea level, the relation of E_0 to N_μ is given by

$$E_0(\mathrm{eV}) = 1.08 \times 10^{17}\, (N_\mu/10^6)^{1.22} \qquad \text{(from (HP))}$$

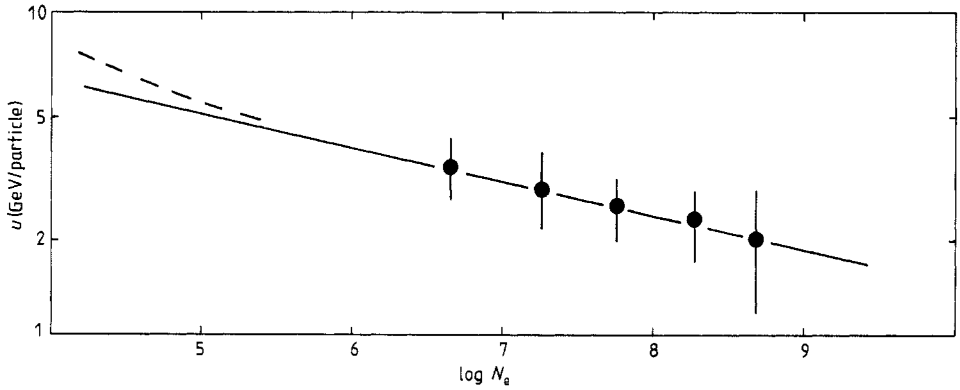

Figure 7. The conversion factor u used to derive the E_0 spectrum from the N_e spectrum.

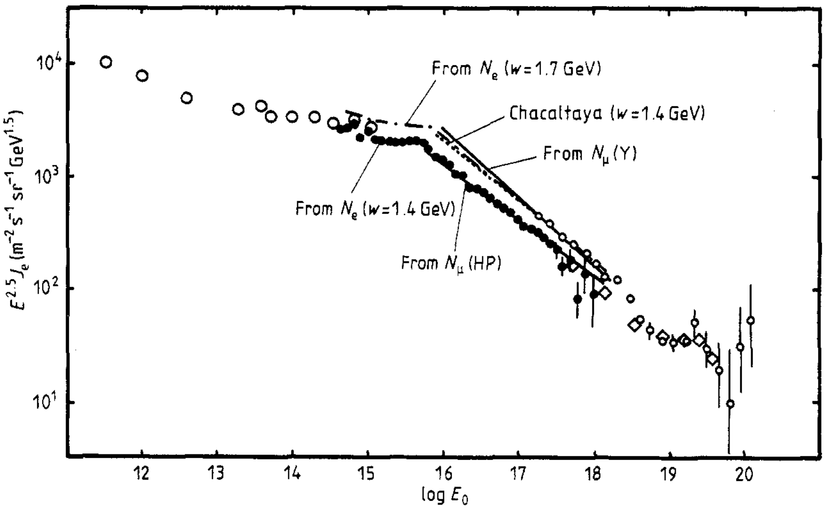

Figure 8. The differential primary spectra obtained from electron and muon size spectra are compared with the earlier results compiled by Hillas (1983). ●, Present experiment; ○, 'Proton' experiments; o, Haverah Park; ◇, Yakutsk.

and

$$E_0(\text{eV}) = (1.46 \pm 0.5) \times 10^{17} (N_\mu/10^6)^{1.15} \qquad \text{(from (Y)).}$$

By applying these conversion relations to our N_μ spectrum we obtain the primary spectra shown by the full curves in figure 8.

4.5. Comparison of the present energy spectrum with others

The agreement of the primary energy spectra derived from the N_e and N_μ spectra is satisfactory. Both methods applied to the present derivation are accepted to good primary energy estimators, independent of the hadronic interaction model and primary composition. The present spectrum connects smoothly to the direct measurements obtained with the Proton satellite by Grigorov *et al* (1971) at 10^{15} eV and to the measurement by Efimov *et al* (1982) at 5×10^{17} eV. As far as their spectra are correct, this suggests that the extrapolation of the shape of the longitudinal development curve by Kakimoto *et al* (1983) and the values of w of Hillas (1983) are acceptable. However, the absolute values of the Chacaltaya N_e(max) spectra are larger than that derived from ours. Their E_0 spectrum with $w = 1.4$ GeV is shown by a dotted curve in figure 8.

The fluxes of N_e spectra at Tien-Shan (Kirov *et al* 1981) and Volcano Ranch (Linsley 1973) are a little low to explain the E_0 spectrum with the above assumptions. However, if we use $w = 1.7$–2.0 GeV (summary of various simulations; Linsley and Hillas 1981), their N_e spectrum can be fitted to the primary spectrum mentioned above, in which case our spectrum is shifted to the chain curve in figure 8.

We have not taken the effect due to the variance α of the values of w or $S(600)$ into account in deriving the primary spectrum, since the factor $\exp(\frac{1}{2}\alpha^2 y^2)$ is smaller than the discrepancies in the values of w and the relation between E_0 and $S(600)$ among various authors.

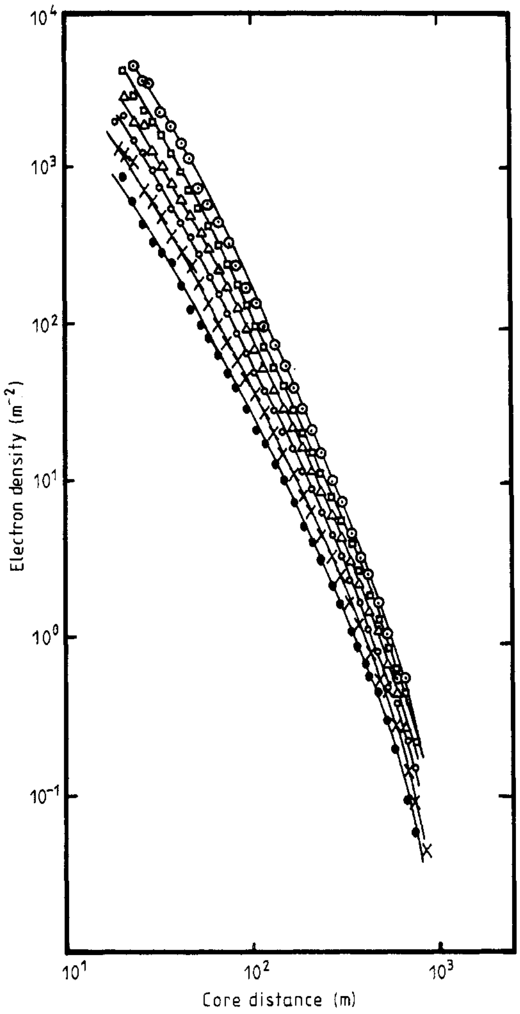

Figure 9. The lateral distribution of electrons at various electron sizes (⊙, log $N_e = 7.8–8$, 3.0%; □, 7.6–7.8, 12.1%; △, 7.4–7.6, 32.3%; ○, 7.2–7.4, 32.3%; ×, 7.0–7.2, 16.3%; ●, 6.7–7.0, 4.0%) for a fixed muon size ($N_\mu = 10^{5.8}–10^{6.0}$). (sec θ= 1.0–1.1.)

4.6. Implications of the spectrum

We have not observed any significant change of slope above the 'knee' in either the electron or muon size spectrum. This result is most easily understood if a single-mass component is dominant in the primary beam or the relative intensities of the main component fluxes do not change appreciably between 10^{16} and 10^{18} eV. This is because the N_e spectrum at Akeno altitude is more sensitive to proton showers than to heavy primary showers, and *vice versa* for the N_μ spectrum. On the other hand, a compilation of most measurements of the size spectrum shows the 'knee' almost at the same size ($\sim 10^6$) irrespective of the observation level (see figure 5). This cannot be understood with a single-mass component and suggests that the primaries are a mixture of the various mass components, unless the knee is due to the change in the nuclear interaction. The details should be discussed together with the energy dependence of other quantities, such as fluctuations of electron size and muon size, fluctuations in the depth of shower maximum, and so on.

5. Conclusions

(i) The vertical electron size spectrum at 920 g cm^{-2} is

$$J(N_e)\,dN_e = (2.80 \pm 0.08) \times 10^{-13}\,(N_e/10^6)^{-\gamma}\,dN_e\ \mathrm{m^{-2}\,s^{-1}\,sr^{-1}}$$

where $\gamma = 2.48 \pm 0.09$ between $10^{5.0}$ and $10^{6.0}$ and $\gamma = 2.83 \pm 0.04$ between $10^{6.0}$ and $10^{8.0}$.

(ii) The vertical muon size spectrum at 920–1020 g cm^{-2} is

$$J(N_\mu)\,dN_\mu = (3.08 \pm 0.17) \times 10^{-16}\,(N_\mu/10^6)^{-3.44 \pm 0.09}\,dN_\mu\ \mathrm{m^{-2}\,s^{-1}\,sr^{-1}}$$

between $10^{5.0}$ and $10^{6.7}$.

(iii) No significant change of slope can be observed in either the electron or muon size spectrum beyond the corresponding energy 10^{16} eV.

(iv) The differential energy spectrum of total particles is expressed by

$$J(E_0)\,dE_0 = (4.0\text{–}5.0) \times 10^{-23}(E_0/10^{15.67})^{-\gamma}\,dE_0\ \mathrm{m^{-2}\,s^{-1}\,sr^{-1}}$$

where $\gamma = 2.62 \pm 0.12$ ($10^{14.5}$–$10^{15.67}$ eV) and 3.02 ± 0.05 ($10^{15.67}$–10^{18} eV).

(v) The conversion factor from N_μ ($\geqslant 1$ GeV at Akeno level) to E_0 is expressed by

$$E_0(\mathrm{eV}) = 1.17 \times 10^{17}\,(N_\mu/10^6)^{1.21} \qquad 10^5 \leqslant N_\mu < 10^{6.7}$$

if the present primary spectrum from N_e is accepted.

(vi) In order to convert N_e at Akeno level to primary energy conventionally, the following relation can be used:

$$E_0(\mathrm{eV}) = 3.9 \times 10^5 \leqslant N_\mu < 10^{6.7}$$

Acknowledgments

The authors wish to thank Messrs Y Hirabayashi, K Hoji, F Ishikawa, K Mesuda, Y Ohno, H Ohoka, M Shimizu and Y Takei for their help in constructing the air-shower array and Mrs R Torii for her help in the analysis and preparation of the typescript. They are grateful to Professor G Tanahashi and Drs M Daigo, N Hasebe, M Honda and N Jogo for their contributions to the experiment. They also thank P K MacKeown for his advice on this paper. The data analysis was performed on FACOM M180-II AD at the Computer Room of the Institute for Nuclear Study, University of Tokyo.

References

Acharya B S *et al* 1981 *Proc. 17th Int. Conf. on Cosmic Rays, Paris* **9** 162

Asakimori K *et al* 1982 *J. Phys. Soc. Japan* **51** 2059

Bagge E R *et al* 1977 *Proc. 15th Int. Conf. on Cosmic Rays, Plovdiv* **12** 24

Bower A J *et al* 1981 *Proc. 17th Int. Conf. on Cosmic Rays, Paris* **9** 166

—— 1983 *J. Phys. G: Nucl. Phys.* **9** L53

Danilova T V *et al* 1977 *Proc. 15th Int. Conf. on Cosmic Rays, Plovdiv* **8** 129

Diminstein O S *et al* 1977 *Proc. 15th Int. Conf. on Cosmic Rays, Plovdiv* **8** 154

Efimov N N *et al* 1981 cited by Hillas (1983)

Glushkov A V *et al* 1979 *Proc. 16th Int. Conf. on Cosmic Rays, Kyoto* **8** 158

Greisen K 1968 *Ann. Rev. Nucl. Sci.* **10** 63

Grigorov N L *et al* 1971 *Proc. 12th Int. Conf. on Cosmic Rays, Hobart* **5** 1746

Hara T *et al* 1979 *Proc. 16th Int. Conf. on Cosmic Rays, Kyoto* **8** 135
—— 1983a *Proc. 18th Int. Conf. on Cosmic Rays, Bangalore* EA1.2-13
—— 1983b *Phys. Rev. Lett.* **50** 2058
Hillas A M 1979 *Proc. 16th Int. Conf. on Cosmic Rays, Kyoto* **8** 7
—— 1981 Rapporteur paper *Proc. 17th Int. Conf. on Cosmic Rays, Paris* **13** 69
—— 1983 *Proc. Cosmic Ray Workshop, University of Utah* p 16
Horton L *et al* 1983 *Proc. 18th Int. Conf. on Cosmic Rays, Bangalore* **6** 124
Jogo N 1981 *Doctor Thesis* University of Tokyo
Kakimoto F *et al* 1981 *Proc. 17th Int. Conf. on Cosmic Rays, Paris* **11** 254
Kawakami S *et al* 1983 Private communication
Kiraly P *et al* 1971 *J. Phys. A: Gen. Phys.* **4** 367
Kirov N *et al* 1981 *Proc. 17th Int. Conf. on Cosmic Rays, Paris* **2** 109
Lapointe M *et al* 1968 *Can. J. Phys.* **46** S68
Linsley J 1973 *Proc. 13th Int. Conf. on Cosmic Rays, Denver* **5** 3207
Linsley J and Hillas A M 1981 *Proc. Paris Workshop on Cascade Simulations* (Texas Center for the Advancement of Science and Technology)
Nagano M *et al* 1984 *J. Phys. Soc. Japan* **53** 1667
Vernov S N *et al* 1968 *Can. J. Phys.* **46** S197